



Relationship between branching density and crystalline structure of A- and B-type maize mutant starches

Catherine Gérard ^a, Véronique Planchot ^{a,*}, Paul Colonna ^a, Eric Bertoft ^b

^a INRA, BP 71627, F-44316 Nantes, France

^b Department of Biochemistry and Pharmacy, Åbo Akademi University, Biocity, PO Box 66, FIN-20521 Turku, Finland

Received 25 November 1999; accepted 10 January 2000

Abstract

Amylopectin from two double maize mutant starches of A-crystalline (*wxdu*) and B-crystalline type (*ae wx*) was subjected successively to hydrolysis involving alpha and beta amylases, which isolated clusters and all branching zones of clusters (BZC). Enzymatic analysis together with ionic and size-exclusion chromatography revealed the structural features of the clusters and BZC and their role in starch crystallization. A-type clusters were larger ($\overline{dp}_n > 80$) and contained more (but shorter) chains than B-type clusters. The BZC of A-type starch was also larger, but with a shorter distance between the branching points than in B-type BZC. A-type clusters had a densely packed structure and B-type a poorly branched structure. Models for the structure of A- and B-type clusters are presented, and a hypothesis for the influence of cluster geometry on crystallization is proposed. © 2000 Elsevier Science Ltd. All rights reserved.

Keywords: Starch mutant; Amylopectin; Cluster structure; Crystallization; Maize; Amylases

1. Introduction

Starch, the main storage carbohydrate of plants, accounts for 50–80% of dry weight in the storage organs of higher plants. Basically, starch consists of two major polymers, amylose and amylopectin. Amylose is essentially a linear macromolecule composed of α -(1 → 4)-

linked glucosyl units, whereas amylopectin is a branched macromolecule with α -(1 → 6) branches in the α -(1 → 4)-linked glucosyl chains [1]. Depending on their botanical origin, native starches display different diffraction patterns [2], an A-type for normal starches and a B-type for tuber starches. Molecular modelling has shown that the organized molecular structure of glucans with α -(1 → 4) linkages, having the lowest energy, is based on double helices, regardless of the allomorphic type (A- or B-) [3]. The differences between the two allomorphs relate to the packing of double helices in the crystal unit cell and the quantity of water molecules stabilizing these double helices. In the B-type structure, double helices are packed in a hexagonal unit cell in which each has three neighbours [4], an arrangement generating a central chan-

Abbreviations: wx, waxy; du, dull; ae, amylose extender; BZC, branching zone of clusters; dp, degree of polymerization; \overline{dp}_n , average degree of polymerization; CL, average chain length; ECL, average external chain length; ICL, average internal chain length; XL, very large; L, large; M, medium; S, small; XS, very small; XXS, smallest; NC, average number of chains; CIR, cupric ion reduction; HPAEC–PAD, high-performance anion exchange chromatography with pulsed amperometric detection.

* Corresponding author. Fax: +33-240-675167.

E-mail address: planchot@nantes.inra.fr (V. Planchot)

nel containing 36 water molecules per unit cell. In the A-structure, double helices are packed in a monoclinic unit cell in which each has six neighbours [5], an arrangement corresponding to a densely packed structure with only four water molecules per unit cell.

The A-type is favoured thermodynamically, and the B-type kinetically [6]. The structure of the A-type is obtained preferentially under conditions of high crystallization temperature, high polymer concentration and short chain length [7]. The length of the amylopectin short chains might also be a determining factor for crystal structure. An A-type diffraction diagram has been obtained for glucose chains with degrees of polymerization (dp) of 10–12 and a B-type for higher degrees [8]. However, as few chains *in vivo* have less than dp 12, their presence is unlikely to influence the whole starch crystallization process. Moreover, as these results were obtained *in vitro* and from linear chains, the exact origin of crystal expression during biosynthesis of the starch granule in a specific allomorphic type is still a matter of debate. Hizukuri [9] has shown *in vivo* that amylopectin molecules in the A-type starches have shorter constitutive chains and larger numbers of short-chain fractions than those in the B-type starches. However, many studies have been based on a thermodynamic approach or on the structural features of whole amylopectin [6–9], and the possible influence of the structural features of clusters on starch crystallization has not been considered.

From a genetic point of view, maize has been the plant system most often studied to understand starch biosynthesis¹. Maize mutant starches are numerous and cover a broad range of granular and macromolecular struc-

tures, making it possible to study the influence of amylose and amylopectin on granule organization and the relative arrangement of these glucans within granules.

A main target of the present study was to investigate the fine structure of amylopectin from A-type (*wxdu*) and B-type (*aewx*) double-mutant maize starches in order to determine how the distance between branching points in a cluster is related to the crystallization pattern of the chain arrangement.

2. Results and discussion

General features of wxdu and aewx starches.—Both starch samples studied were constituted solely of amylopectin, which allowed us to avoid any influence of amylose in the results. The chain-length distributions of *wxdu* and *aewx* amylopectins were studied after debranching with isoamylase (EC 3.2.1.68). In *wxdu* and *aewx* amylopectins, average chain length (CL) values were 17.3 and 28.8, respectively (Table 1), as determined with the cupric ion reduction (CIR) method. Although the *wxdu* CL value (17.3) was lower than values determined by size-exclusion chromatography [12–14] (ranging from 20.1 to 21.3), it was concordant with the *wx* CL value determined by Yun and Matheson [15] using the CIR method. In agreement with these authors, the *aewx* CL value was 28.8, i.e., higher than that of *wxdu* and similar to the *ae* amylopectin CL value (29.4) [16].

The difference in chain-length distributions between *wxdu* and *aewx* amylopectin was confirmed by HPAEC–PAD analysis (Fig. 1(a,b)): *aewx* amylopectin was composed of fewer short chains and more long chains than *wxdu* amylopectin. Moreover, the top fractions of *aewx* and *wxdu* short chains corresponded to dp 15 and dp 12, respectively, which is consistent with classical observations of longer short chains in *aewx* than in *wxdu* amylopectin [17,18]. The limits of beta amylolysis were 58 and 55% for *wxdu* and *aewx*, respectively, a difference possibly due to the reduced number of chains in *aewx* as compared with *wxdu* amylopectin. External chain length (ECL) and internal chain length (ICL)

Table 1
Structural characteristics of *wxdu* and *aewx* amylopectins

	CL	%β-Limit	ECL ^a	ICL ^b
<i>wxdu</i>	17.3	58	12.0	4.3
<i>aewx</i>	28.8	55	17.8	10.0

^a ECL = CL × (%β-limit/100) + 2.

^b ICL = CL – ECL – 1.

¹ For a review, see Refs. [10,11].

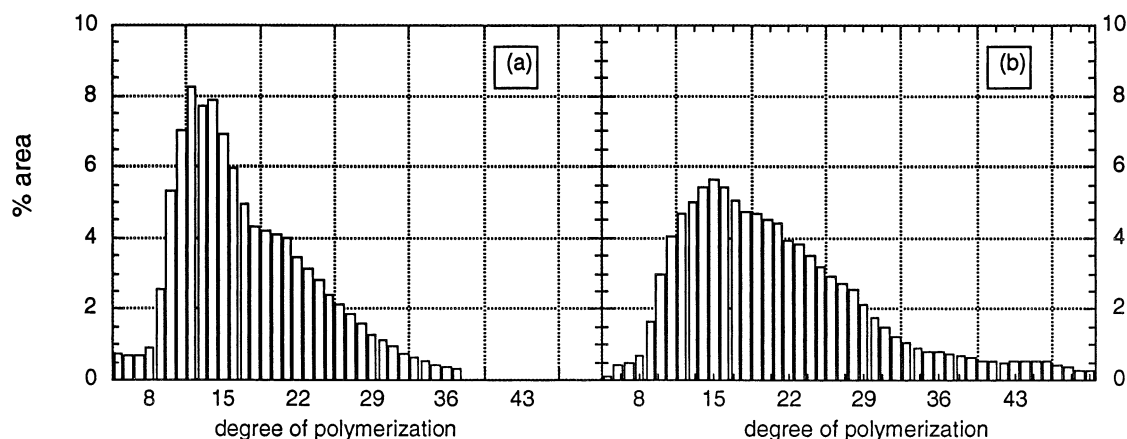


Fig. 1. Analysis by HPAEC–PAD of debranched amylopectin with isoamylase: *wxdu* (a) and *aewx* (b) presented as % area vs. the dp of carbohydrates.

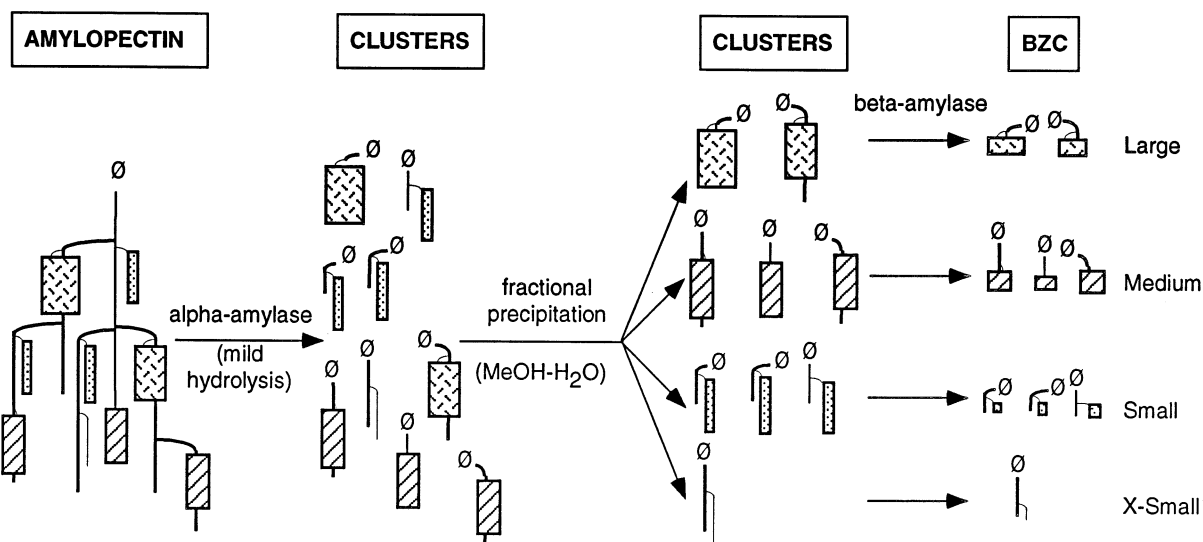


Fig. 2. Methods used to isolate clusters and the BZC for complete characterization of amylopectin structure. MeOH–H₂O ratios are indicated in Table 2.

were determined on the basis of the β -limit and CL values (Table 1). ECL and ICL values for *aewx* amylopectin were six glucosyl units higher than for *wxdu*. Thus, constitutive chains of *aewx* amylopectin were longer than those of *wxdu* amylopectin, and the average distance between branching points was greater because of the higher ICL value. Compared with ECL and ICL values for most amylopectins (from maize, *waxy* maize or potato) [19], those for *wxdu* amylopectin (12.0 and 4.3, respectively) were shorter, though similar to those for highly branched *waxy* rice amylopectin [20]. This suggested that the *wxdu* sample had a similar highly branched structure.

Fine structure of wxdu amylopectin.—The clusters and branching zones of clusters (BZC) were isolated successively by hydrolysis with alpha amylase (EC 3.2.1.1) and beta amylase (EC 3.2.1.2) (Fig. 2). The first step consisted of mild hydrolysis using alpha amylase from *Bacillus amyloliquefaciens*, an enzyme containing nine subsites around the catalytic site [21]. As enzyme attack is faster when all subsites are filled with α -D-glucosyl residues, the initial attack on amylopectin occurs in the external chains, which are hydrolysed preferentially into maltohexaose [21] and independently in longer internal chain segments between branches [22]. Accordingly, alpha amylase from *B. amyloliquefaciens* was used to cut

long internal chains and isolate the clusters. Different methanol–water ratios were used for fractional precipitation of clusters depending on their size. Fractions of large (L), medium (M), small (S) and very small (XS) clusters were obtained. Extensive hydrolysis with beta amylase was performed on each fraction to reduce ECL to 2 or 3 units.

Production and characterization of wxdu α -dextrins. To define the optimal experimental conditions for cluster isolation, hydrolysis of wxdu amylopectin was performed on an analytical scale using alpha amylase of *B. amyloliquefaciens*, and the reaction was followed by size-exclusion chromatography on a Sepharose CL 6B column. Hydrolysis kinetics was similar to that obtained with waxy rice [20], waxy maize [23] or potato amylopectin [24]. As distinct intermediate products were formed from amylopectin, the kinetics was characteristic of a non-random attack. After 2 h of hydrolysis, α -dextrins showed a narrow size distribution with a top fraction around dp 140. Hydrolysis (2 h) was performed on a preparative batch to obtain α -dextrins, which were subsequently precipitated by 5 volumes of methanol (Fig. 3(a)). High-performance anion exchange chromatography with pulsed amperometric detection (HPAEC–PAD) analysis showed that the methanol supernatant

consisted essentially of maltohexaose, as previously reported [21,22], although an equal quantity of maltoheptaose was detected. HPAEC–PAD analysis was not suitable for the detection of high-molecular-weight material.

To obtain complete characterization of wxdu clusters of different sizes, the fractionation of α -dextrins was carried out using MeOH–H₂O ratios ranging from 0.9:1 to 5:1 (Table 2). The first precipitation, performed with a 0.9:1 ratio, produced the largest α -dextrins (XL). Large (L) and medium (M) α -dextrins were then obtained using 1.7:1 and 3:1 ratios, respectively. The residual supernatant contained smaller α -dextrins. The methanol in this supernatant was evaporated and the dextrins were concentrated and freeze-dried. A new fractional precipitation performed on these residual α -dextrins, using MeOH–H₂O ratios of 3:1 and 5:1, produced small (S) and very small (XS) dextrins, respectively. The final supernatant contained the smallest dextrins (XXS), which were freeze-dried after methanol evaporation and XXS concentration.

The proportions of XL, L, M, S, XS and XXS clusters in wxdu amylopectin were 19, 38, 13, 12, 4 and 14%, respectively. The size distribution of each fraction was determined

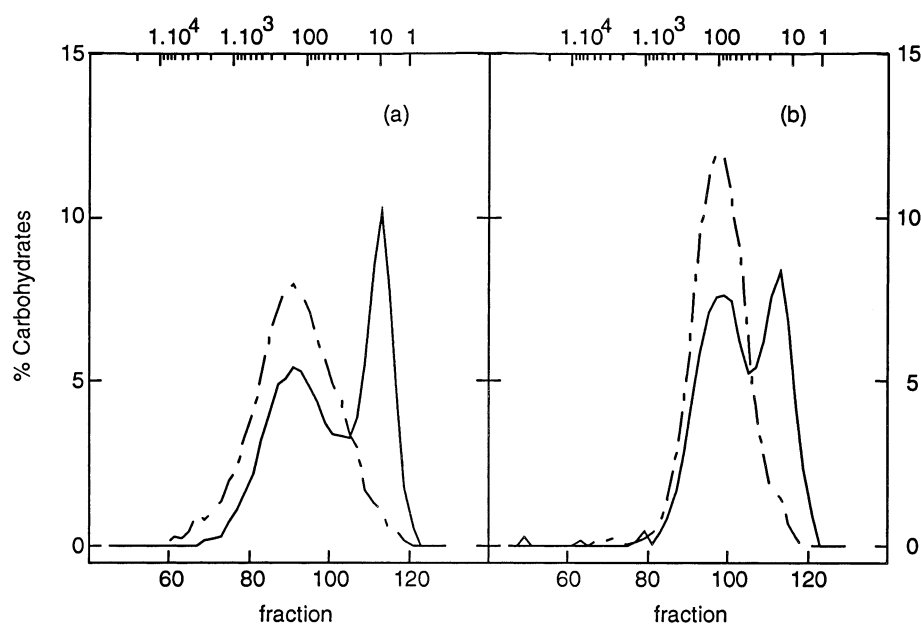


Fig. 3. Analysis on a Sepharose CL 6B column of (a) wxdu and (b) aewx hydrolysates after 2 h of alpha amylolysis before (—) and after precipitation with 5 vol of methanol (---).

Table 2
Fractional precipitation and structural characteristics of *wxdu* and *awwx* α -dextrins

	MeOH–H ₂ O ratio	Yield ^a (%)	dp Range ^b	\overline{dp}_n ^b	\overline{CL} ^c	\overline{ECL} ^d	\overline{NC} ^e	Branch density ^f	β -Limit ^g (%)
<i>wxdu</i>									
XL	0.9:1	19	50–5000	213	9.1	5.3	23.4	10.5	36.6
L	1.7:1	38	50–1000	172	10.4	6.1	16.6	9.1	39.4
M	3:1	13	20–350	84	11.2	7.5	7.5	7.7	49.5
S	supernatant, 3:1	12	10–250	58	11.5	8.3	5.0	6.9	54.4
XS	supernatant, 5:1	4	10–100	35	11.0	9.4	3.2	6.3	67.4
XXS	supernatant	14	10–50	15					77.8
<i>awwx</i>									
L	1:1	18	25–450	123	12.6	8.5	9.8	7.2	51.2
M	2.5:1	58	20–300	68	13.4	8.7	5.1	6.0	50.1
S	supernatant, 5:1	14	10–100	39	15.7	12.2	2.5	3.8	65.1
XS	supernatant	9	10–50	15					91.7

^a Yields from the original mixture after 2 h of alpha amylolysis and precipitation in 5 vol of methanol.

^b From size-exclusion chromatography on Sepharose CL 6B.

^c Calculated after isoamylase debranching.

^d $\overline{ECL} = \overline{CL} \times (\% \beta\text{-limit}/100) + 2$.

^e Average number of chains = $\overline{dp}_n/\overline{CL}$.

^f $(\overline{NC} - 1)/\overline{dp}_n \times 100$.

^g Estimated from size-exclusion chromatography on PD10.

by size-exclusion chromatography on Sepharose CL 6B (Fig. 4(a), Table 2). Seventy percent of the clusters (XL, L and M) showed a \overline{dp}_n value above 80. In comparison, the α -dextrins produced by *waxy* maize [22] and *waxy* rice amylopectins [20] all had $\overline{dp}_n > 80$ after 1 h of amyolysis.

Wxdu clusters had a \overline{CL} value lower than that of the original *wxdu* amylopectin, ranging from 9.1 to 11.5 (Table 2). With *waxy* maize [22] and potato amylopectins [24], the decrease in the \overline{CL} value of α -dextrins was mainly due to a shortening of the external chains, although \overline{ICL} was also reduced. At a certain point during hydrolysis, the \overline{ECL} of *waxy* maize [22] and potato amylopectins [24] was approximately similar in all α -dextrin fractions, regardless of size. However, in the case of *wxdu* clusters, \overline{ECL} increased notably with decreasing cluster size, suggesting a difference (not clearly defined) in the fine structure of *wxdu* amylopectin as compared with that of *waxy* maize and potato samples. Due to the increase in \overline{ECL} , the beta amyolysis limit increased from 36.6% for the largest to 77.8% for the smallest clusters.

The average number of chains per cluster (\overline{NC}) was 23.4 and 16.6 for XL and L clusters, respectively (Table 2). The density of branches

was high in these clusters (9.1–10.5% of the glucosyl residues were branched), but decreased to 6.3 for the XS clusters.

Characterization of wxdu β -limit dextrins. β -Limit dextrins prepared from each cluster type induced the isolation of BZC, i.e., cluster regions where all branching points are located. The size distribution of *wxdu* BZC was determined by size-exclusion chromatography on Sepharose CL 6B (Fig. 4(c)). The largest BZC (M, L and XL) had a \overline{dp}_n of 38–94, and the smallest ones (S and XS) had a $\overline{dp}_n \leq 25$ (Table 3). \overline{CL} , determined after debranching with pullulanase (EC 3.2.1.41), ranged from 4.7 to 5.4. The number of chains per BZC ranged from 7.6 to 18.7 in M, L and XL fractions, and from 2.6 to 5.2 in XS and S fractions. As expected, these values were consistent with the number of chains on the α -dextrins. The size of the β -limit dextrins or the BZC of *wxdu* amylopectins was similar to that of ϕ , β -limit dextrins of *waxy* rice amylopectin [20], although branch density was greater (17–19) than in *waxy* rice clusters (13–14.5) [25].

Characterization of wxdu β -limit dextrins by additional alpha amyolysis. Alpha amyolysis was performed again, in the same conditions as above (0.03 U of alpha amylase/mL), for each of the β -limit dextrins. After 2 h of alpha

amyolysis, no significant changes in size distribution and \overline{dp}_n values were observed, indicating that no long internal chains remained and that true clusters had been isolated.

To obtain a more complete description of cluster and BZC geometry, β -limit dextrans were treated with an alpha amylase solution 100-fold more concentrated (3 U/mL), which produced dextrans practically resistant to further attack [20]. The size distribution of these dextrans ($dp < 80$) was determined by size-exclusion chromatography on a Superdex 30 column (Fig. 5(a)). As the smallest single branched dextrin known to be produced by

the alpha amylase of *B. amyloliquefaciens* is 6²- α -maltosyl-maltotriose [26,27], the material obtained with a $dp < 5$ could be considered as linear. Extensive alpha amyolysis of *wxd* BZC produced only a small amount of this linear material, which was significant for a small proportion of long internal chains in the BZC. However, there was a high proportion of branched dextrans ($dp > 5$), called building blocks [20]. After extensive alpha amyolysis, the BZC of the original *wxd* amylopectin had a \overline{dp}_n value of 13.3 and a broad distribution of building blocks, with two main populations above and below dp 20. XL, L, and M *wxd*

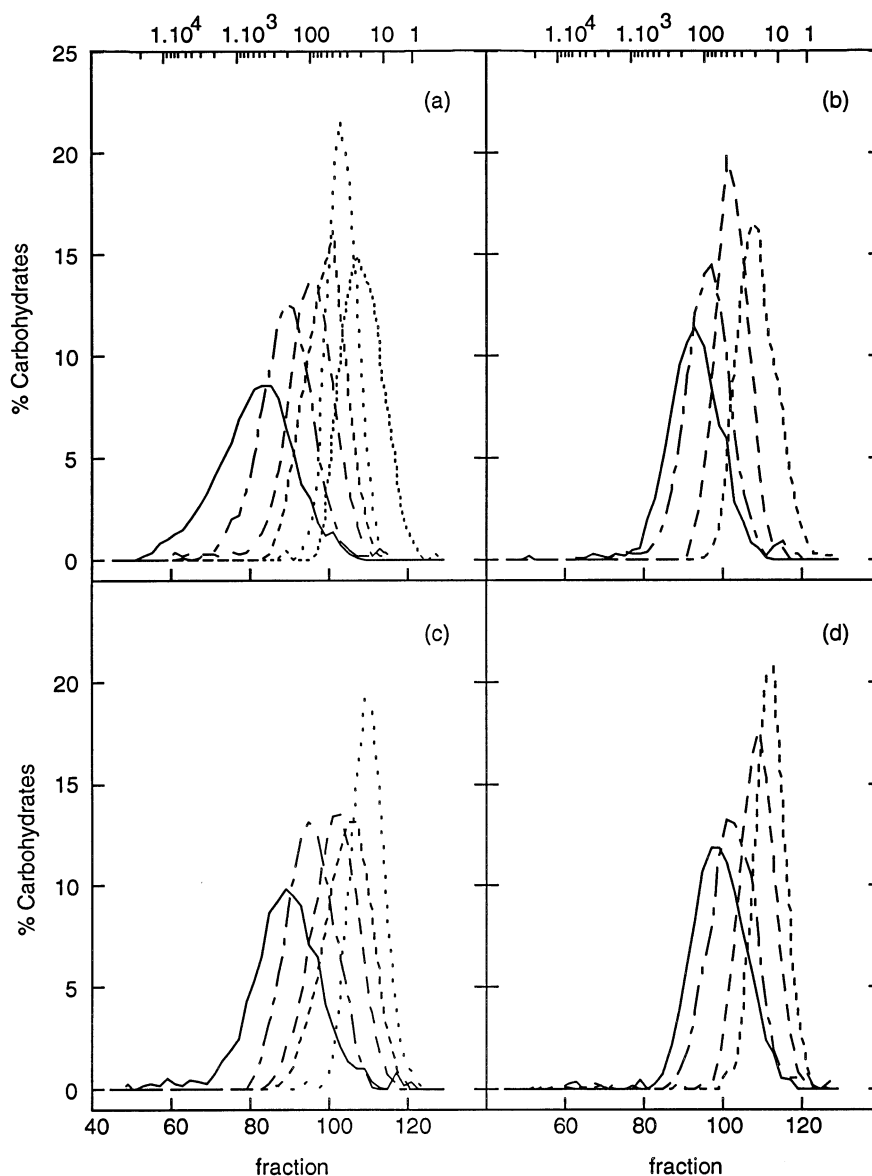


Fig. 4. Fractionation on a Sepharose CL 6B column of *wxd* α -dextrans (a) and β -limit dextrans (c): —XL, — — —L, — — —M, — — —S, ····XS, ·····XXS and of *aewx* α -dextrans (b) and β -limit dextrans (d): —L, — — —M, — — —S, — — —XS.

Table 3
Structural characteristics of *wxdu* and *aewx* β -limit dextrins

	dp Range ^a	\overline{dp}_n ^a	\overline{CL} ^b	\overline{NC} ^c	Branch density ^d
<i>wxdu</i>					
XL	30–1525	94	5.0	18.7	18.8
L	25–460	84	5.3	15.8	17.6
M	10–230	38	5.0	7.6	17.4
S	10–180	25	4.7	5.2	16.8
XS	5–55	14	5.4	2.6	11.4
<i>aewx</i>					
L	10–300	47	5.7	8.2	15.3
M	10–180	32	6.0	5.3	13.4
S	6–70	17	5.3	3.2	12.9
XS	5–30	11	5.1	2.2	10.9

^a From size-exclusion chromatography on Sepharose CL 6B.

^b Calculated after pullulanase debranching.

^c Average number of chains = $\overline{dp}_n/\overline{CL}$.

^d $(\overline{NC} - 1)/\overline{dp}_n \times 100$.

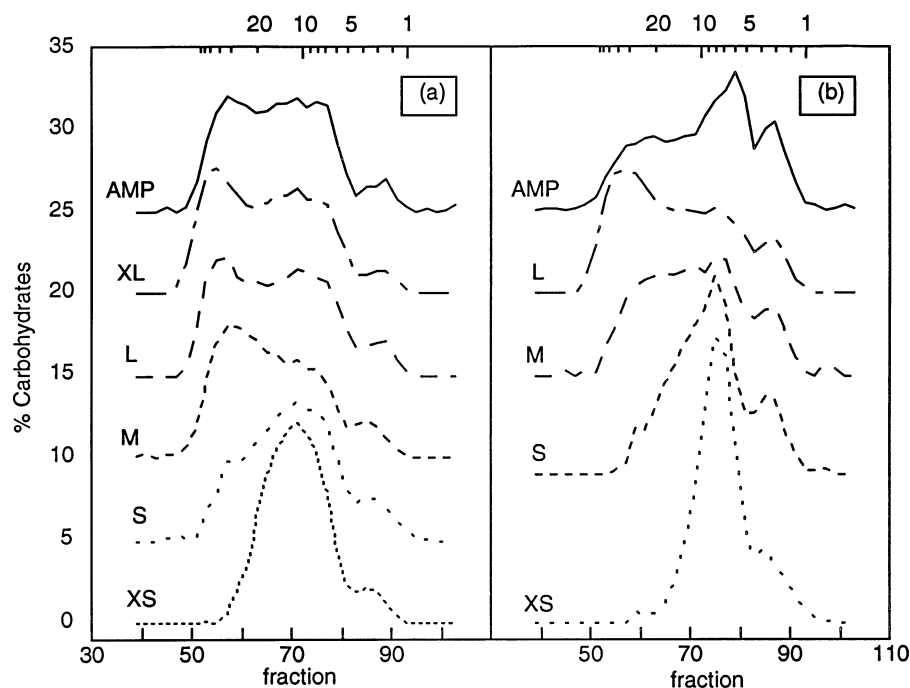


Fig. 5. Fractionation on a Superdex 30 column of hydrolytic mixtures of β -limit dextrins after extensive alpha amylolysis for 3 h: (a) *wxdu* amylopectin and fractions, (b) *aewx* amylopectin and fractions.

BZC also showed a broad distribution of building blocks, but with fewer $dp < 20$ dextrins than in the original amylopectin. The proportion of big building blocks was high in large *wxdu* BZC, and the size distribution was similar to that of the large ϕ , β -limit dextrins in *waxy* rice [20]. XL, L, and M BZC had an average number of 5.7, 5.6 and 2.4 branched

blocks, respectively, with $\overline{dp}_n > 13.6$ (Table 4), confirming the highly branched structure. The density of branched building blocks, which is the same as the proportion of glucosyl residues binding a building block within a cluster [20], was 6.1–6.7. Small *wxdu* BZC (S and XS) showed narrower distributions, with few dextrins of $dp > 20$ and few blocks (< 2)

with small \overline{dp}_n values (~ 11), but with comparatively high block density. In comparison, *waxy* rice amylopectin showed clusters with a branched building block density of 5.3–6.7 [20].

Fine structure of aewx amylopectin

Production and characterization of aewx α -dextrins. On an analytical scale, when alpha amylase of *B. amyloliquefaciens* was used, the hydrolysis of *aewx* amylopectin showed kinetics similar to that of *wxdu* amylopectin, except that *aewx* α -dextrins displayed a narrower size distribution after 2 h of hydrolysis, with a top fraction of around dp 90 (Fig. 3(b)). The position of this top fraction was 50 glucosyl units lower than with the *wxdu* sample. For the same hydrolysis time, *aewx* amylopectin produced smaller α -dextrins and less low-molecular-weight material than *wxdu* amylopectin. In order to compare the geometry of

aewx and *wxdu* clusters, hydrolysis was also stopped after 2 h in a preparative batch of *aewx* amylopectin. The mixture of *aewx* α -dextrins was precipitated using 5 volumes of methanol (Fig. 3(b)). HPAEC–PAD analysis showed that maltohexaose and maltoheptaose were the main oligomers of the methanol supernatant.

Different MeOH–water ratios were used to fractionate α -dextrins (Table 2). The precipitations performed with 1:1 and 2.5:1 ratios produced large (L) and medium (M) dextrins, respectively, and the residual supernatant contained the smaller α -dextrins. The methanol in the supernatant was evaporated, and the α -dextrins were concentrated and freeze-dried. Another fractional precipitation performed with these residual α -dextrins (5:1 MeOH–water ratio) yielded small dextrins (S). The final supernatant contained the smallest α -dextrins

Table 4

Composition of building blocks in branching zones of clusters (BZC) of *wxdu* and *aewx* starches and in *waxy* rice ϕ , β -limit dextrins obtained by extensive alpha amylolysis

	\overline{dp}_n blocks ^a	\overline{dp}_n whole mixture ^b	Number of blocks ^c	Block density ^d
<i>wxdu</i>				
Amylopectin	13.3	10.3		
XL	14.6	11.4	5.7	6.1
L	13.6	9.9	5.6	6.7
M	14.7	11.1	2.4	6.3
S	11.6	8.2	1.9	7.6
XS	10.6	8.9	1.2	8.6
<i>aewx</i>				
Amylopectin	10.2	6.7		
L	14.1	9.4	2.9	6.2
M	11.5	7.9	2.3	7.2
S	9.6	7.0	1.4	8.2
XS	7.9	6.0	1.2	10.9
<i>waxy</i> rice ^e				
Amylopectin	12.8	8.4		
10.1 ^f	17.1	11.8	5.8	5.3
11.1 ^f	12.7	9.2	3.1	6.7
3 ^g	13.8	8.5	4.2	6.4

^a From size-exclusion chromatography on Superdex 30 (*wxdu* and *aewx*) or Superdex 75 (*waxy* rice).

^b Includes small linear dextrins with $dp < 5$.

^c Average number of branched blocks included in clusters.

^d (Number of blocks/ \overline{dp}_n of BZC fraction) $\times 100$.

^e From Ref. [20].

^f Obtained from an original 3-h alpha amylolysis mixture, from which samples 10.1 and 11.1 with \overline{dp}_n 110 and 47, respectively, were isolated.

^g Obtained from an original 1-h alpha amylolysis mixture, from which sample 3 with \overline{dp}_n 66 was isolated.

(XS), which were freeze-dried after methanol evaporation. The proportions of L, M, S, and XS clusters in *aewx* amylopectin were 18, 58, 14 and 9%, respectively.

The size distribution of each fraction was determined (Fig. 4(b), Table 2). *Aewx* clusters showed narrower size distributions than *wxdu* clusters, and only L *aewx* clusters had $\overline{dp}_n > 80$ ($\overline{dp}_n = 123$). The M fraction composed the greater part (58%) of *aewx* clusters, with a \overline{dp}_n value of 68. S and XS *aewx* clusters, with \overline{dp}_n values of 39 and 15, respectively, were similar to XS and XXS *wxdu* clusters. On the whole, *aewx* clusters were smaller than *wxdu* clusters, with CL values of 12.6–15.7 indicative of longer chains than in *wxdu* clusters. The number of chains per cluster for L, M and S fractions was 9.8, 5.1 and 2.5, respectively. Branch density was less than in *wxdu* clusters of comparable size, ranging from 3.8 in smaller clusters to 7.2 in larger ones. As the main fraction of *wxdu* clusters (L) showed an NC value of 16.6 and a branching density of 9.1, *aewx* clusters in general were apparently less branched than *wxdu* clusters. *Aewx* clusters were also less branched than *waxy* rice clusters [20], except for the L *aewx* fraction which had an NC value similar to that obtained for fractions 11.1 and 3 of *waxy* rice. For potato amylopectin [24], the size of cluster units was similar to that of M and S *aewx* clusters, ranging from \overline{dp}_n 30–70.

As *aewx* clusters showed longer ECL values and contained fewer branching points, their β amylolysis limits were greater than those of *wxdu* clusters, ranging from 51.2% for large ones (L) to 91.7% for the smallest ones (XS).

Characterization of *aewx* β -limit dextrins. The size distribution of *aewx* BZC was determined by size-exclusion chromatography (Fig. 4(d), Table 3). The \overline{dp}_n values of *aewx* BZC were lower (11–47) than those of *wxdu*. Conversely, large and medium *aewx* BZC showed CL values of 5.7 and 6.0, respectively, which were higher (5.0–5.3) than those for XL, L and M *wxdu* BZC. As expected, the number of chains was similar in *aewx* BZC and clusters. The branching density of *aewx* BZC decreased from 15.3 to 10.9, confirming that there were fewer branching points in *aewx* than *wxdu* clusters.

Characterization of *aewx* β -limit dextrins by additional alpha amylolysis. Alpha amylolysis was performed on each BZC fraction in the initial conditions (0.03 U/mL). As for *wxdu*, this additional hydrolysis produced no significant changes in the size distribution of BZC, indicating that no longer internal chains existed in *aewx* BZC and that true clusters had been isolated by hydrolysis of the preparative batch of *aewx* amylopectin.

Extensive (3 h) alpha amylolysis (3 U/mL) was performed on *aewx* β -limit dextrins to compare the geometry of *aewx* and *wxdu* BZC, and the size distribution of the dextrins was determined (Fig. 5(b)). The proportion of linear material ($dp < 5$) produced by extensive alpha amylolysis on BZC and amylopectin β -limit dextrin was higher for *aewx* than *wxdu*, indicating that greater ICL in *aewx* samples allowed amylolysis and the production of more linear material [20]. The building blocks of *aewx* amylopectin β -limit contained a very high proportion of dextrins within the 5–20 dp range, and the size distribution was completely different than that of *wxdu* blocks. The \overline{dp}_n value of *aewx* amylopectin β -limit dextrin was 10.2. The number of branched blocks produced by *aewx* BZC was lower (1.2–2.9) than in *wxdu* samples (Table 4).

The size distribution of the building blocks showed different profiles, depending on the *aewx* BZC fraction subjected to extensive alpha amylolysis. Extensive alpha amylolysis of L *aewx* BZC produced blocks with a size distribution and a \overline{dp}_n value (14.1) similar to those of XL, L, and M *wxdu* blocks, with a high proportion of $dp > 20$ dextrins. M *aewx* BZC produced only 2.3 branched blocks, whose size distribution showed fewer $dp > 20$ and more dp 5–20 dextrins. The \overline{dp}_n value of M *aewx* branched blocks was reduced to 11.5. The building blocks of S and XS *aewx* BZC contained only $dp < 20$ dextrins and showed \overline{dp}_n values of 9.6 and 7.9, respectively. Thus, the proportion of building blocks with $dp < 20$ became greater as the size of *aewx* BZC decreased, whereas the size distribution of building blocks from XL, L and M *wxdu* BZC was similar, with a high proportion of $dp > 20$ dextrins. S and XS *wxdu* BZC produced a larger amount of dextrins with $dp < 20$, but

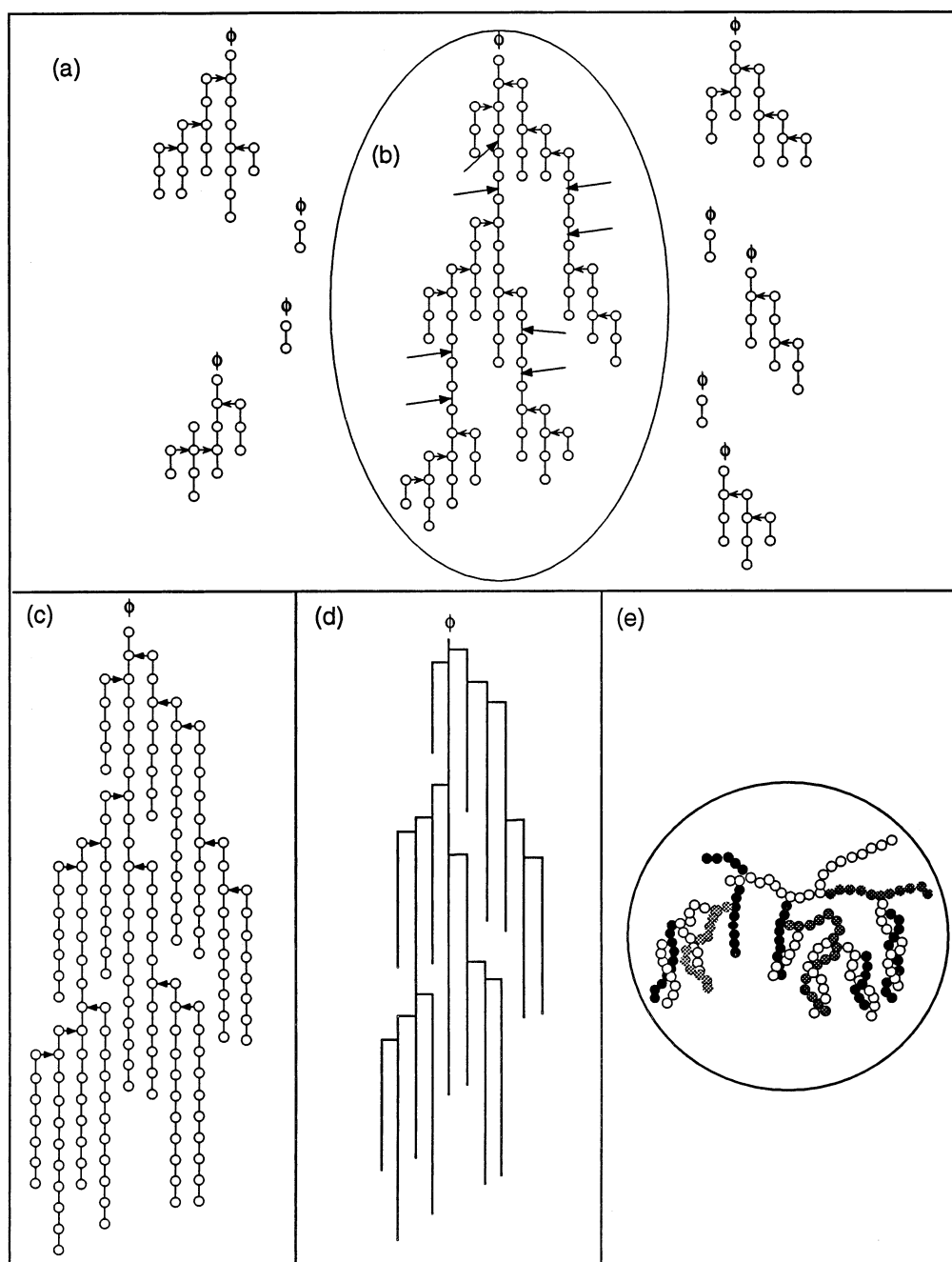


Fig. 6. Proposed structure of a large *wxdu* cluster: (a) building blocks, (b) branching zone of the cluster (arrow indicates extensive alpha amylolysis attack), (c) a cluster with all glucosyl units, (d) a cluster in symbolized form and (e) a cluster as an organized structure.

these fractions had a broader size distribution than S and XS *aewx* BZC.

These results indicate that L *aewx* BZC and XL, L and M *wxdu* BZC had similar structures characterized by large building blocks, numerous chains, high branch density and few linear dextrans ($dp < 5$), whereas M *aewx* BZC, the major cluster component in this

amylopectin, displayed a different structure characterized by fewer chains and longer distances between branching points.

Construction of wxdu and aewx clusters.— Figs. 6 and 7 show the proposed geometry of *wxdu* and *aewx* clusters based on L *wxdu* and M *aewx* clusters, whose proportions were the highest in each amylopectin (38 and 58%,

respectively). The models are average ones, and cluster distribution within the amylopectin is still undetermined.

The first step in calculating the geometry of the *wxd* cluster consisted in drawing the building blocks produced by extensive alpha amylolysis of BZC (Fig. 6(a)). The building blocks were then arranged in the BZC with respect to its dp_n (Fig. 6(b)). Chains were

homogeneously elongated from the BZC (Fig. 6(c)). Fig. 6(d) shows an L *wxd* cluster in symbolized form without glucosyl units. The same cluster (Fig. 6(e)) is shown as it might appear in the form of an organized structure within the granule (participating in crystalline and amorphous lamellae). The structure of the *wxd* cluster is very dense, with numerous chains and short distances between branching

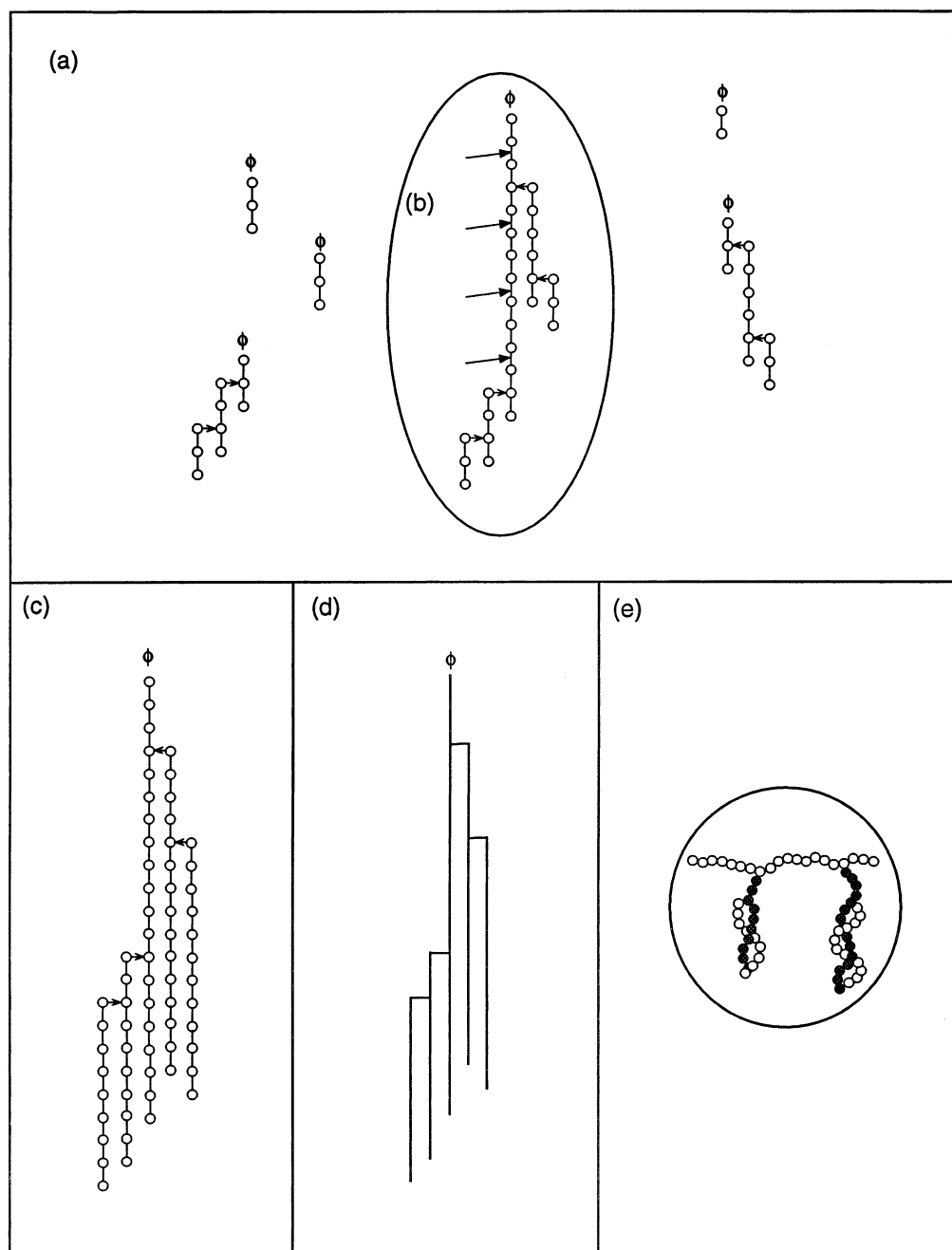


Fig. 7. Proposed structure of a medium *aewx* cluster: (a) building blocks, (b) branching zone of the cluster (arrow indicates extensive alpha amylolysis attack), (c) a cluster with all glucosyl units, (d) a cluster in symbolized form and (e) a cluster as an organized structure.

points. With respect to the homogeneity of the size distribution of building blocks for each *wxdu* BZC fraction, XL, L and M *wxdu* clusters showed the very same densely packed structure, with various numbers of chains per cluster.

A proposed structure for the M *aewx* cluster (Fig. 7) is based on the same approach as for the L *wxdu* cluster. M *aewx* clusters showed few chains and long distances between branching points. However, the size distribution of building blocks and the branching density suggested that L *aewx* clusters had the same densely packed structure as the major clusters of *wxdu* amylopectin.

During starch biosynthesis, granule formation requires both elongation and branching activities involving several enzymes [10,11]. Biosynthesis of *wxdu* starch occurs in the absence of some elongation activities. As a result, branching activity is favoured and biosynthesis produces the very densely packed structure described above. Conversely, during *aewx* starch biosynthesis, one of the branching activities responsible for amylopectin short chains is deficient, resulting in the poorly branched structure of *aewx* amylopectin.

Hypothesis for the influence of cluster geometry on crystallization.—If it is assumed that S, XS and XXS *wxdu* clusters are too small to affect the overall crystallinity process, then the allomorphic type of *wxdu* starch must be due to the crystallization of very large (XL), large (L) and medium (M) clusters, which are composed of numerous chains and show a short distance between branching points, as reported by Bertoft et al. [20] and Bertoft and Koch [25] for the structure of *waxy* rice amylopectin. Thus, it is likely that the crystallization of these highly packed structures results in a 100% A type. A cluster geometry with numerous chains and a short distance between branching points induces crystallization in the A allomorphic type.

It may also be assumed that small (S) and very small (XS) *aewx* clusters are not involved in the organization of *aewx* starch. The polymorphic type of *aewx* starch is due to the crystallization of M and L *aewx* clusters that form 58 and 18%, respectively, of the total amylopectin structure. According to these

proportions, the crystallization of M clusters accounts for 76% [$= 58/(18 + 58) \times 100$] of the total *aewx* organization, 24% being due to crystallization of L clusters [$= 18/(58 + 18) \times 100$]. Our investigations showed that *aewx* L clusters had a densely packed structure with a short distance between branching points, as in the case of *wxdu* clusters. The crystallization of such clusters produces the A allomorphic type, accounting for the presence of 25% of A-type crystallites in *aewx* starch. The remaining M *aewx* clusters were smaller but similar to clusters from potato amylopectin [24]. Their poorly branched structure, with a long distance between branching points, would result in crystallization into a B allomorphic type. As *aewx* starch was 75% B-type and 25% A-type, there seems to be a relationship between cluster geometry and the crystallization of chain arrangement. The crystallization of starch into a specific allomorphic type is influenced by the fine structure of amylopectin.

3. Conclusions

Chain-length distribution of amylopectin is known to influence the polymorphic type of the granule. However, the results of our study indicate that the distance between two α -(1 \rightarrow 6) linkages and the branching density inside each cluster are also determining factors for the development of crystallinity in the starch granule. Clusters composed of numerous short chains and characterized by a short distance between successive chains within the amylopectin molecule produce densely packed structures. These structures appear to crystallize into the A allomorphic type. Clusters with fewer but longer chains and BZC with a long distance between branching points produce a poorly packed structure and subsequently crystallize into the B allomorphic type.

The results presented here emphasize the role of starch branching enzymes, which should be considered not only for their chain length specificity, but also for their α -(1 \rightarrow 6) linkage distribution. Previous mathematically based studies on starch granule crystallinity [3–5,37] have proposed models of branched macromolecule conformation around and

within the crystal. However, these models have not been confirmed by experimental results. The present study provides experimental results for comparison with these models.

4. Experimental

Materials.—*Aewx* starch and fresh *wxdu* maize grains were supplied by Limagrain Genetics (France). Fresh *wxdu* maize grains were vacuum-dried at 30 °C, and *wxdu* starch was isolated in the laboratory according to a procedure derived from Ref. [28] and recovered with a yield of 97%. Alpha amylase of *B. amyloliquefaciens*, with an activity of 600 U/mg [29], was purchased from Boehringer-Mannheim, and beta amylase from sweet potato was obtained from Sigma (25,000 U/mL). Isoamylase of *Pseudomonas amyloclavata* (59,000 U/mg) and pullulanase of *Klebsiella pneumoniae* (40 U/mg) were purchased from Hayashibara.

Starch isolation and amylopectin fractionation.—*Aewx* and *wxdu* starches were defatted by Me₂SO treatment according to Ref. [30], except that the precipitate was washed with EtOH and acetone and air-dried under a hood overnight. The defatted *aewx* and *wxdu* starches were recovered at yields of 97 and 96%, respectively. As *wxdu* starch was pure amylopectin, no further fractionation was necessary. A part of the *aewx* amylopectin was poorly branched, containing linear chains (14%) long enough to form complexes with iodine (Gérard et al., unpublished data). This part was removed, and the pure *aewx* amylopectin was fractionated. The starch was autoclaved for 25 min at 130 °C (2.5 mg/mL) under nitrogen to avoid degradation, and amylopectin molecules with long linear chains and few branchings were then precipitated for 72 h by addition of thymol (1 mg/mL), yielding 87% pure amylopectin.

Crystalline structure.—*Wxdu* starch showed the classical cereal A-type, whereas *aewx* starch was of B-type. Moreover, the results obtained with multilinear regression on the diffracted intensities indicated that *aewx* starch was also composed of 25% A-type crystallites [31]. A high and similar crystallinity

level ($47\% \pm 4\%$) was found for both *wxdu* and *aewx* starches.

Characterization of amylopectin.—Stock solutions of *wxdu* and *aewx* amylopectins were obtained by dissolution in 90% Me₂SO (50 mg/mL) for three days at room temperature (rt). These solutions were diluted 20-fold with water to determine the beta amylolysis limit. Working solutions were then obtained by adding 0.1 M NaOAc buffer, pH 4.8, (2.4 mL) to aliquots (0.1 mL) of stock solutions. Beta amylolysis was performed by adding 5 µL of beta amylase to 1 mL of the working solution. After incubation overnight at rt, the maltose produced was analyzed enzymatically using NADP⁺-coupled reactions [22,32]. Total carbohydrate content was measured with phenol-H₂SO₄ [33]. To estimate CL, stock solutions were diluted 10-fold with water, and 0.1 M NaOAc buffer, pH 3.5, (0.2 mL), water (0.5 mL) and isoamylase (2 µL) were added to aliquots (1.2 mL) of these solutions. After incubation overnight at rt, the mixture was boiled, and the reducing value determined [34]. The CL was calculated as total carbohydrate/reducing value. The average ECL and ICL were calculated from beta amylolysis limit values [22] ($ECL = CL \times (\% \beta\text{-limit} / 100) + 2$; $ICL = CL - ECL - 1$).

Production of amylopectin β-limit dextrin.—*Aewx* and *wxdu* amylopectins were dissolved in 90% Me₂SO (50 mg/mL) for 3 days at rt. The solutions were then diluted 10-fold with 0.1 M NaOAc buffer, pH 4.8, and beta amylase was added (2.5 U/mg substrate). The mixture was incubated overnight at rt and then boiled for 2 min. The sample was dialysed against water and freeze-dried. Beta amylolysis was repeated once in the same conditions.

Production of α-dextrins.—*Wxdu* and *aewx* amylopectins (2 g) were dissolved in 90% Me₂SO (40 mL) and stirred for 3 days at rt. The solutions were then diluted with water (320 mL) and treated at 25 °C with alpha amylase (40 mL) in 0.01 M NaOAc buffer, pH 6.5, using a final concentration of 0.03 U of enzyme and 5 mg of substrate/mL. After 2 h, the reaction was stopped with 5 M KOH (10 mL). Intermediate α-dextrins were precipitated with 5 vol of MeOH, washed with MeOH, dissolved in boiling water for 30 min

and freeze-dried. α -Dextrins were then fractionated into a series of precipitates of different size distributions using increasing MeOH–water ratios of 0.5:1 to 5:1, as described previously [23].

Characterization of α -dextrins.— α -Dextrins were directly dissolved in hot water for 30 min at concentrations of 1.2–1.5 mg/mL, and their molecular-weight distribution was then determined on a Sepharose CL 6B column. To estimate $\overline{\text{CL}}$, α -dextrins (1 mg) were dissolved in boiling water (0.9 mL) for 15 min, and 0.1 M NaOAc buffer, pH 3.8, (0.1 mL) and isoamylase (2 μ L) were added to this solution. After incubation overnight at 37 °C, reducing value was determined [35], and total carbohydrate was assayed by orcinol–H₂SO₄ [36]. The CL was calculated as total carbohydrate/reducing value.

Production of β -limit dextrins.— α -Dextrins (5 mg/mL) were dissolved in boiling water for 15 min. After cooling, 0.1 M NaOAc buffer, pH 4.8, (0.1 vol) and beta amylase (25 U/mg substrate) were added. The mixture was incubated overnight at rt and then boiled. The maltose was removed using two PD 10 columns, as previously described [20], and beta amyloysis was performed again under the same conditions. The separation of β -limit dextrins from maltose by means of the PD 10 columns allowed the β -limit value of dextrins to be estimated. The final β -limit dextrins were then freeze-dried.

Characterization of β -limit dextrins.— α -Limit dextrins were directly dissolved in hot water for 30 min at concentrations of 1.2–1.5 mg/mL, and their molecular-weight distribution determined on a Sepharose CL 6B column. To estimate average CL, β -limit dextrins (1 mg) were then dissolved in boiling water (0.9 mL) for 15 min. To this solution was added 0.1 M NaOAc buffer, pH 5.5, (0.1 mL) and pullulanase (2 μ L). After incubation overnight at rt, the reducing value was determined [34]. Total carbohydrate was measured with phenol–H₂SO₄ [33], and $\overline{\text{CL}}$ was calculated as total carbohydrate/reducing value.

Alpha amyloysis of β -limit dextrins.— β -Limit dextrins (5 mg) were dissolved in boiling water (0.9 mL) and then treated in a water bath at 25 °C. A solution of alpha amylase

(0.1 mL) in 0.01 M NaOAc buffer, pH 6.5, was added to give a final enzyme concentration of 0.03 U/mL. Aliquots were taken at intervals for analysis by size-exclusion chromatography on a Sepharose CL 6B column. Extensive alpha amyloysis was performed identically, but with concentrations of 2.5 mg of substrate/mL and 3 U of enzyme/mL. The products of extensive alpha amyloysis were analysed on a Superdex 30 column, as described below.

Size-exclusion chromatography.— α -Dextrins and β -limit dextrins were dissolved in hot water (1.2–1.5 mg/mL). The molecular-weight distribution of the dextrins was analysed on a Sepharose CL 6B column, as described previously [20]. The molecular-weight distribution of β -limit dextrins after extensive alpha amyloysis was analysed on a Superdex 30 column with 0.1 M KOH as elution medium. Fractions (0.5 mL) were analysed for carbohydrates using phenol–H₂SO₄ reagent [33]. The columns were calibrated using α -dextrins and β -limit dextrins from *waxy* maize and *waxy* rice starches, which have structures similar to the studied dextrins and are of a known molecular weight. The calibration curves allowed the $\overline{\text{dp}}_n$ of the dextrins to be calculated as $\overline{\text{dp}}_n = 100 / \sum (\% \text{ carbohydrates})_i / \text{dp}_i$, in which $(\% \text{ carbohydrates})_i$ is the relative carbohydrate content and dp_i the degree of polymerization of fraction i .

HPAEC–PAD.—Chromatography was performed on a Dionex BIOLC instrument (Sunnyvale, CA) with a pulsed amperometric detector. Debranched samples (0.6–1.0 mg/mL) were filtered, and an aliquot (25 μ L) was injected onto a CarboPac PA-100 anion exchange column (250 \times 4 mm) coupled to a CarboPac PA-100 guard column. The acetate gradient system included two eluents: 150 mM NaOH (eluent A) and 150 mM NaOH containing 500 mM NaOAc (eluent B). The flow rate was 1 mL/min. The elution gradient was 0–1.3 min, linear gradient from 25 to 34% eluent B; 1.3–6.3 min, linear gradient to 45% eluent B; 6.3–55.7 min, linear gradient to 67% eluent B; finally, 55.7–80.7 min, linear gradient to 90% eluent B and 80.7–90.3 min, linear gradient to 25% eluent B.

Acknowledgements

This work was supported by the European Union, FAIR Program (CT-95-0568). The authors are grateful to Arnaud Messenger from Ulice (France) for providing *wxd* and *aewx* maize samples.

References

- [1] A. Buléon, P. Colonna, V. Planchot, S. Ball, *Int. J. Biol. Macromol.*, 23 (1998) 85–112.
- [2] J.R. Katz, *Z. Phys. Chem.*, 150 (1930) 37–59.
- [3] A. Imberty, H. Chanzy, S. Pérez, A. Buléon, V. Tran, *J. Mol. Biol.*, 201 (1988) 365–378.
- [4] A. Imberty, S. Pérez, *Biopolymers*, 27 (1988) 1205–1221.
- [5] A. Imberty, H. Chanzy, S. Pérez, A. Buléon, V. Tran, *Macromolecules*, 20 (1987) 2634–2636.
- [6] M.J. Gidley, *Carbohydr. Res.*, 161 (1987) 301–304.
- [7] M.J. Gidley, P.V. Bulpin, *Carbohydr. Res.*, 161 (1987) 291–300.
- [8] B. Pfannemüller, *Int. J. Biol. Macromol.*, 9 (1987) 105–108.
- [9] S. Hizukuri, *Carbohydr. Res.*, 141 (1985) 295–306.
- [10] S.G. Ball, *Trends Glycosci. Glycotechnol.*, 7 (1995) 405–415.
- [11] A.M. Smith, *Curr. Opin. Plant Biol.*, 2 (1999) 223–229.
- [12] Y. Ikawa, D.V. Glover, Y. Sugimoto, H. Fuwa, *Starch/Stärke*, 33 (1981) 9–13.
- [13] A.G.W. Bradbury, A.B.T. Bello, *Cereal Chem.*, 70 (1993) 543–547.
- [14] Y.J. Wang, P. White, L. Pollack, J. Jane, *Cereal Chem.*, 70 (1993) 171–179.
- [15] S.-H. Yun, N.K. Matheson, *Carbohydr. Res.*, 243 (1993) 307–321.
- [16] T. Baba, Y. Arai, *Agric. Biol. Chem.*, 48 (1984) 1763–1775.
- [17] H. Fuwa, D.V. Glover, K. Miyaoura, N. Inouchi, Y. Konishi, Y. Sugimoto, *Starch/Stärke*, 39 (1987) 295–298.
- [18] R.C. Yuan, D.B. Thompson, C.D. Boyer, *Cereal Chem.*, 70 (1993) 81–89.
- [19] D.J. Manners, *Carbohydr. Polym.*, 11 (1989) 87–112.
- [20] E. Bertoft, Q. Zhu, H. Andtfolk, M. Jungner, *Carbohydr. Polym.*, 38 (1999) 349–359.
- [21] J. Robyt, D. French, *Arch. Biochem. Biophys.*, 100 (1963) 451–467.
- [22] E. Bertoft, *Carbohydr. Res.*, 189 (1989) 181–193.
- [23] E. Bertoft, L. Spoof, *Carbohydr. Res.*, 189 (1989) 169–180.
- [24] Q. Zhu, E. Bertoft, *Carbohydr. Res.*, 288 (1996) 155–174.
- [25] E. Bertoft, K. Koch, *Carbohydr. Polym.*, 41 (2000) 121–132.
- [26] D. French, E.E. Smith, W.J. Whelan, *Carbohydr. Res.*, 22 (1972) 123–134.
- [27] R.C. Hughes, E.E. Smith, W.J. Whelan, *Biochem. J.*, 88 (1963) 63–64.
- [28] N. Singh, S.R. Eckhoff, *Cereal Chem.*, 73 (1996) 659–667.
- [29] E. Bertoft, R. Manelius, Q. Zhu, *Starch/Stärke*, 45 (1993) 215–220.
- [30] L.A. Belloperez, P. Roger, B. Baud, P. Colonna, *J. Cereal Sci.*, 27 (1998) 267–278.
- [31] C. Gérard, V. Planchot, A. Buléon, P. Colonna, in P. Colonna, S. Guilbert (Eds.), *Biopolymer Science: Food and Non-Food Applications*, INRA, Paris, 1999, pp. 57–63.
- [32] H.O. Beutler, *Methods Enzyme Anal.*, 6 (1984) 119–126.
- [33] M. Dubois, K.A. Gilles, J.K. Hamilton, P.A. Rebers, F. Smith, *Anal. Chem.*, 28 (1956) 350–356.
- [34] S. Waffenschmidt, L. Jaenicke, *Anal. Biochem.*, 165 (1987) 337–340.
- [35] J.D. Fox, J.F. Robyt, *Anal. Biochem.*, 195 (1991) 93–96.
- [36] V. Planchot, P. Colonna, L. Saulnier, in B. Godon, W. Loisel (Eds.), *Guide Pratique d'Analyses dans les Industries des Céréales*, Lavoisier, Paris, France, 1997, pp. 350–353.
- [37] A.C. O'Sullivan, S. Pérez, *Biopolymers*, 50 (1999) 381–390.